Dual-Polarization Radar

from Chapter 7 in Rauber & Nesbitt, Radar Meteorology: A First Course

Z, Z_{DR}, L_{DR}

- L_{DR} is only observed with research radars having a special hardware configuration.
- Z_{HH} and Z_{DR} in rain for specific droplet diameters at different radar wavelengths:

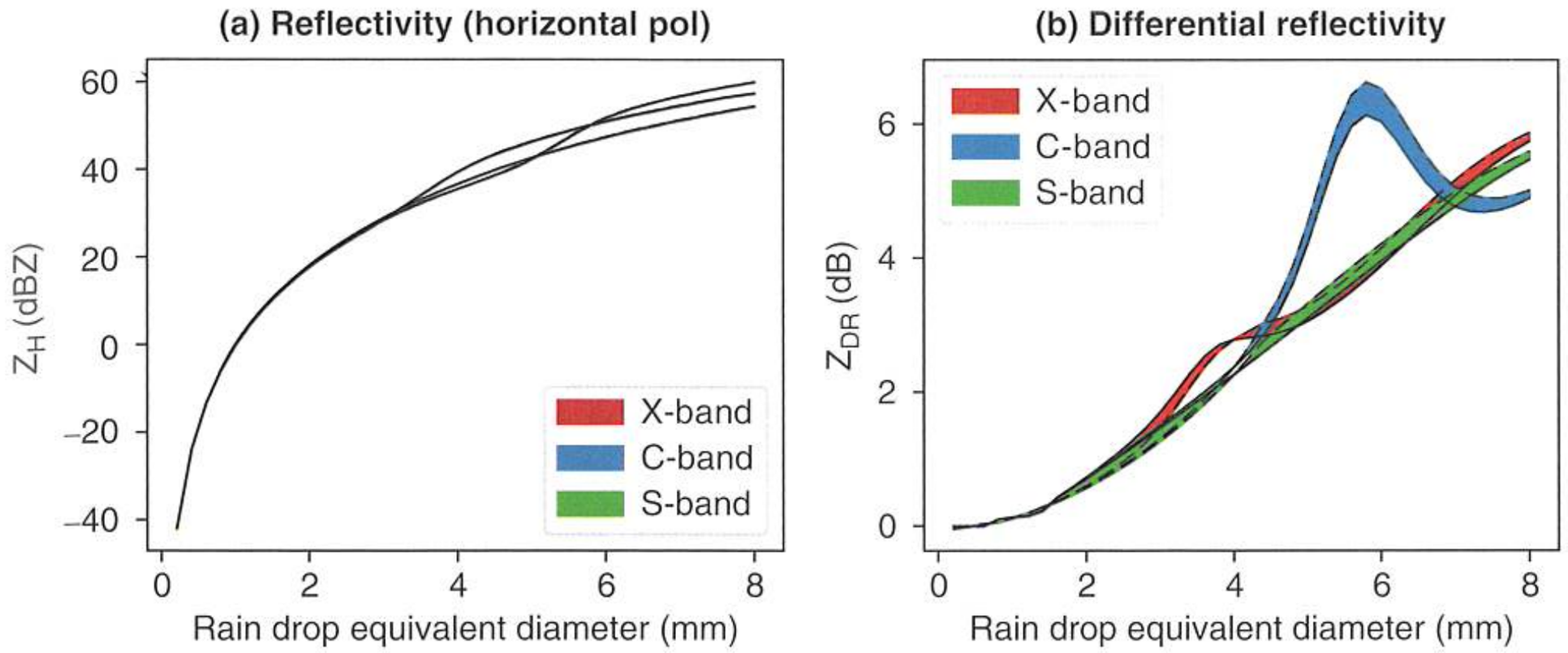

Figure 7.9 T-matrix simulations of a raindrop (a) reflectivity at horizontal polarization and (b) differential reflectivity versus drop equivalent diameter at S-band (green), C-band (blue), and X-band (red). The dashed and solid lines denote different axis ratio parameterizations. Droplet canting was modeled with a Gaussian distribution with a 7° standard deviation

Z, Z_{DR}, L_{DR}

- Z_{DR} measurements in ice and mixed-phase precipitation.

- A common observation in deep convective updrafts containing mixed-phase regions is the Z_{DR} column.

- In pristine ice crystals and snow aggregates, Z_{DR} provides information about the shape and orientation of the particles.

- Complex shapes of dendrites leads to positive $Z_{DR.}$ Dendritic growth layer is -13 to -18 C.

- Aggregates tend to be more spherical and tend to cant/flutter producing Z_{DR} ~ 0 dB.

- In snow, Z_{DR} ~ 0 dB and Z_{HH} > 30 dBZ indicates moderate to heavy snowfall rates.

Polarization and phase

- Phase of received wave differs from that of transmitted wave due to interaction with particles in the radar volume as well as during the propagation along the radar beam's path.

- In a Doppler radar, the phase shift relative to transmitted wave of a number of samples is used to determine the Doppler velocity.

- A dual-pol radar also measures the phase shift of each pulse at each polarization.

- Assume that Doppler phase shift is the same for polarization, the remaining phase shift is due to polarization-dependent interactions with hydrometeors.

Polarization and phase

- ***Propagation differential phase shift*** (ϕ_{DP}):
  - The index of refraction of a medium ($n = c/v_c$) is related to the speed of electromagnetic radiation in that medium. (In a vacuum, $n = 1$.)
  - In water, *n* ~ 8 at S-band: slower propagation. But mixing ratio of water is small, so slowdown is not large.
  - Effects are proportional to water content in radar volume (for a given particle oblateness).

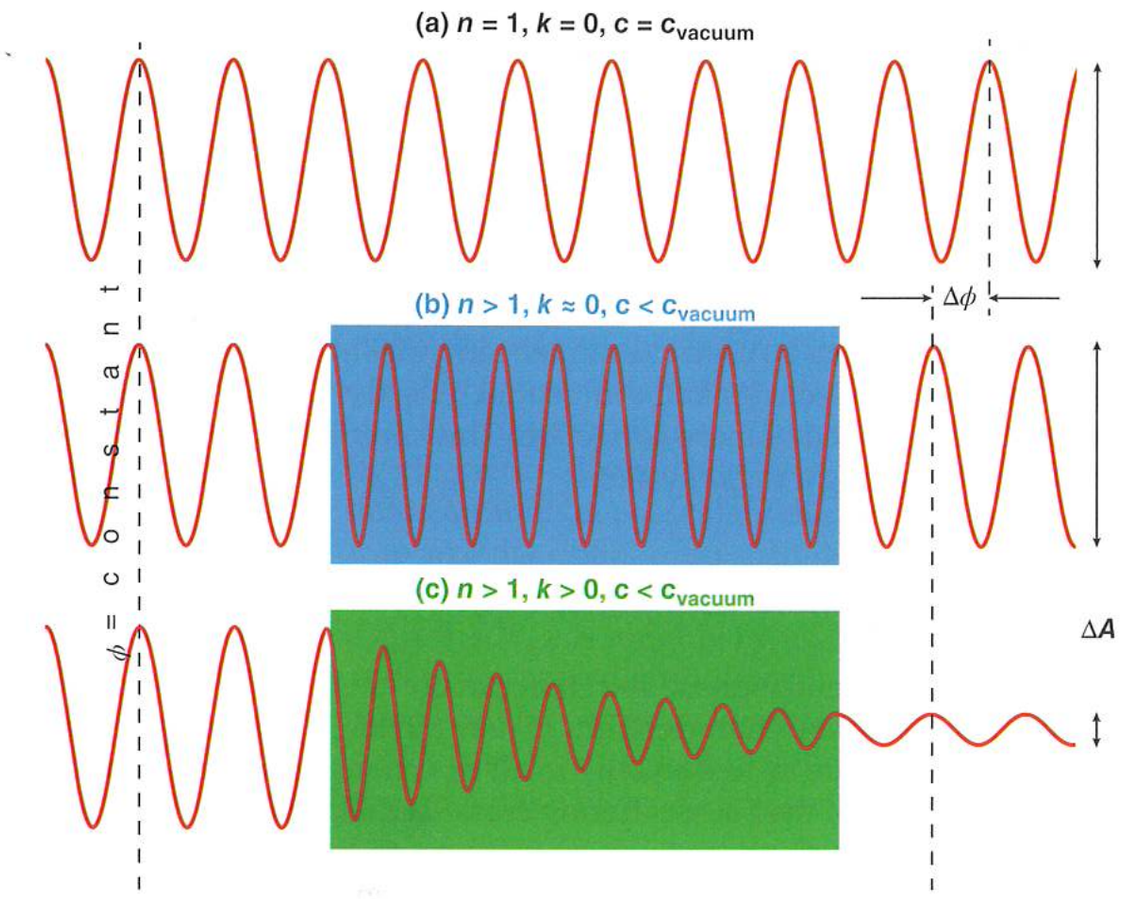

vacuum

slowdown (can measure)

attenuation (can be corrected for)

Figure 7.18 Illustration of the differential phase shift ($\Delta\phi$) and attenuation (ΔA) effects of passing through matter of different complex indices of refraction

Polarization and phase

- ***Specific differential phase*** (K_{DP}):
  - $K_{DP} = \frac{1}{2}\frac{d(\phi_{DP})}{dr}$ ~ range derivative of ϕ_{DP}.

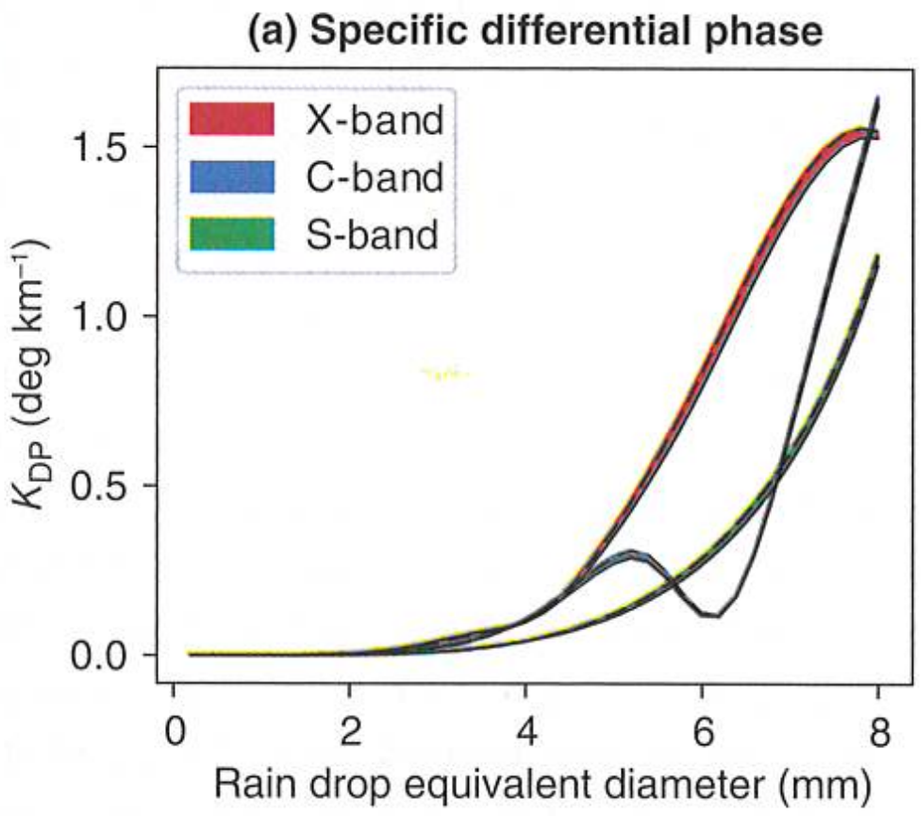

Polarization and phase

- When is K_{DP} significant in real hydrometeors?
  - K_{DP} can be shown to be directly related to mass-weighted droplet axis ratio (“oblateness”).
- K_{DP} ~ number concentration and oblateness of droplets.
- Allows for accurate estimates of liquid water content and precipitation rate.

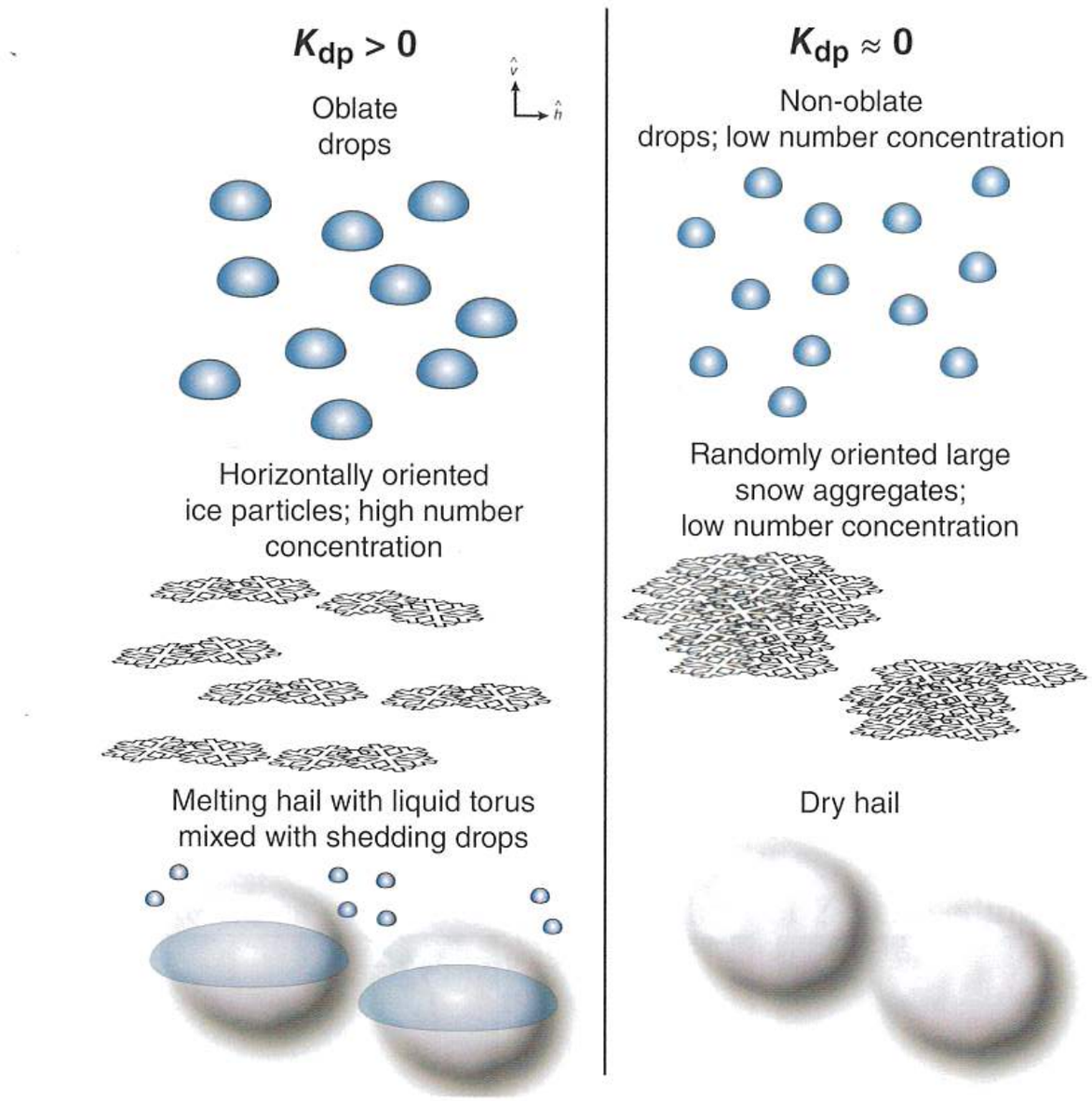

Figure 7.20 Illustration of microphysical factors that, in practice, lead to positive differential phase (left panel) and small to zero differential phase (right panel)

Polarization and phase

- Co-polar correlation coefficient (ρ_{HV})
  - We compare the time series of the complex amplitudes of the returned radar signal at each polarization.
  - Mixtures in sizes and shapes of the particles within a radar volume will lower ρ_{HV}.
  - The tornado debris ball is an example of non-meteorological objects lowering ρ_{HV}.

Polarization and phase

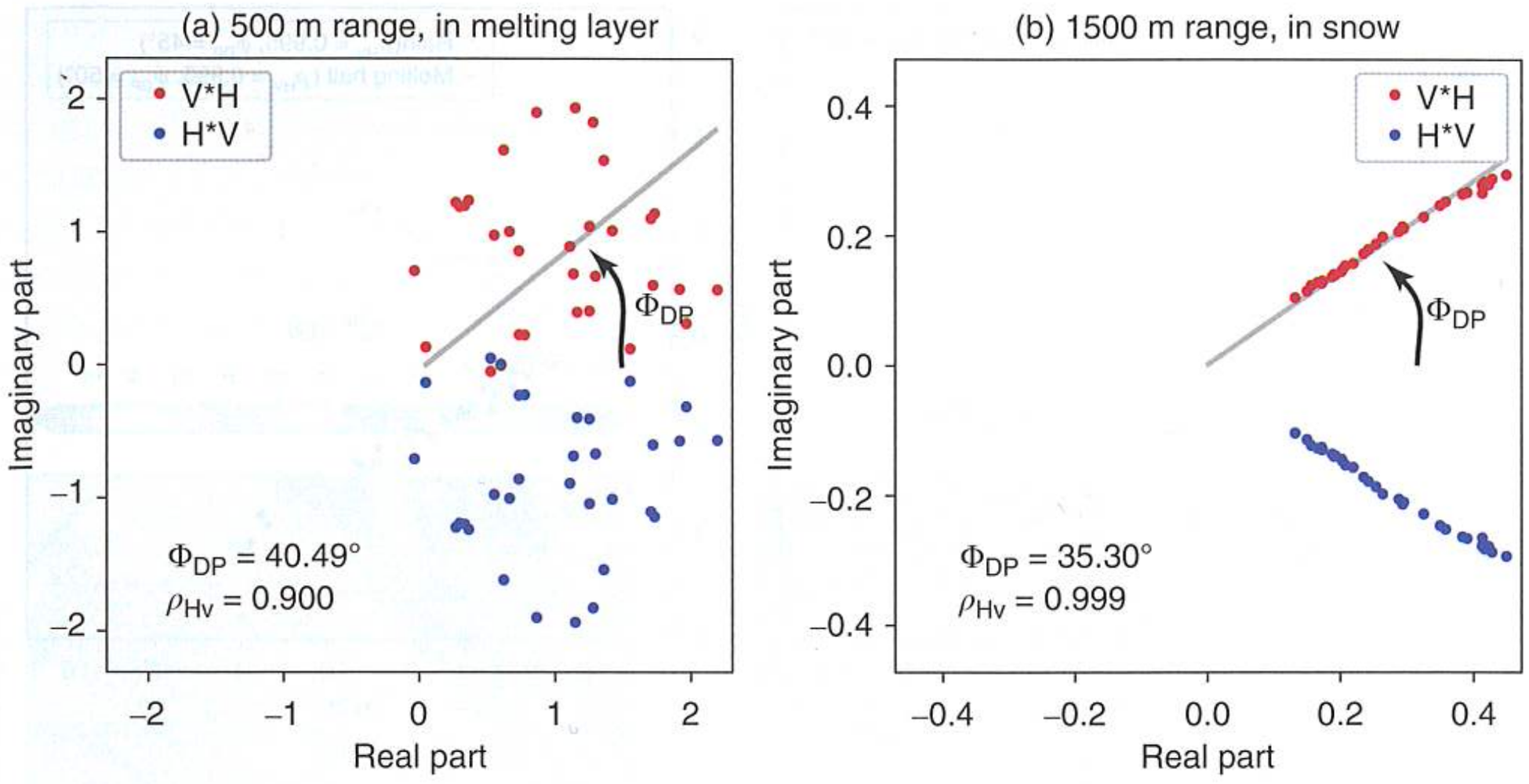

Figure 7.28 Doppler on Wheels (DOW) complex pulse pair time series measurements observed at the University of Illinois at Urbana-Champaign campus from March 3, 2016 at 16:37 UTC. Data from (a) range = 500 m within the bright band and (b) range = 1500 m within snow. The red and blue points show the H*V and V*H points. The angle depicted is an illustration of the estimate differential phase. Thirty-two pulses are shown from each sample

Polarization and phase

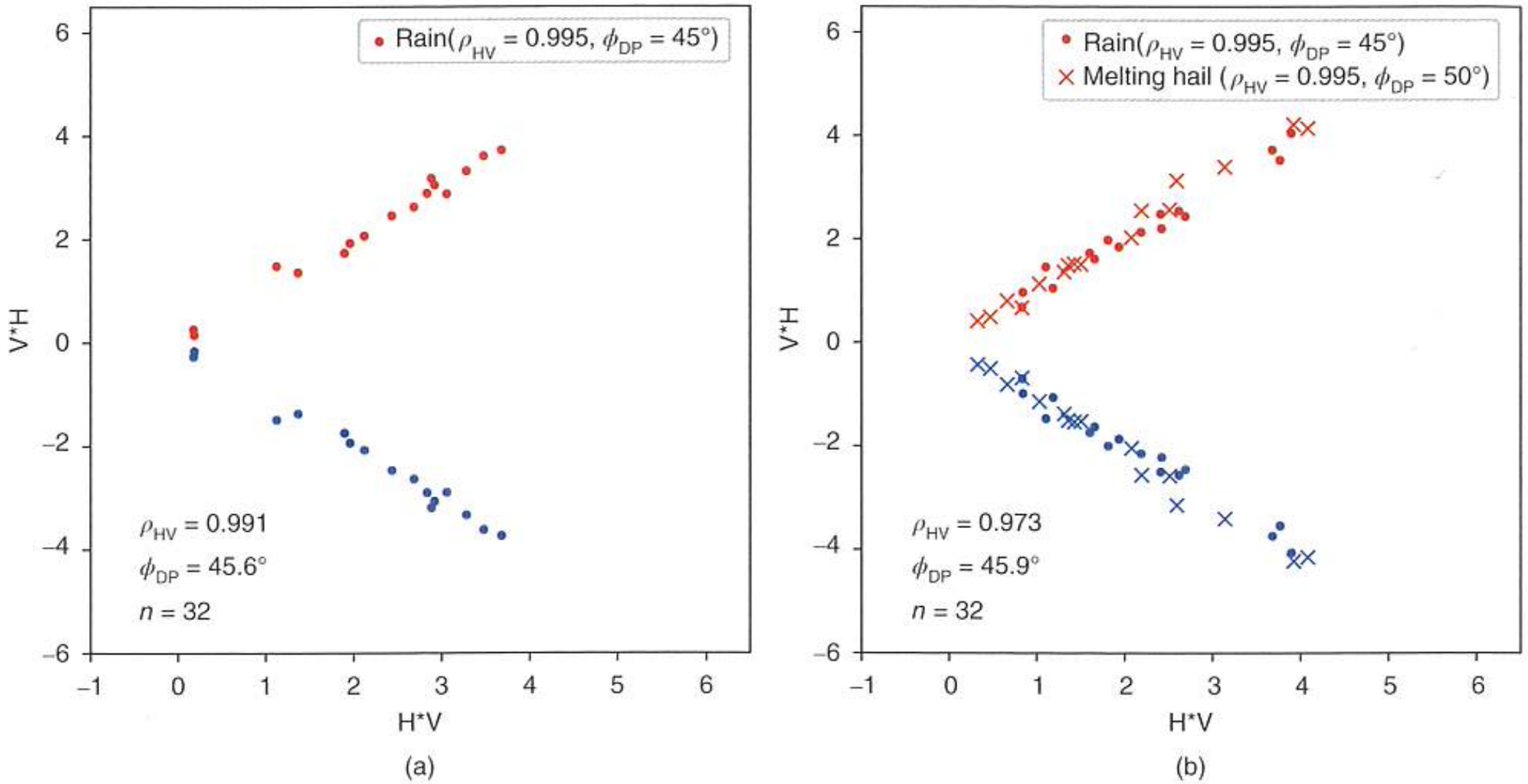

Figure 7.29 Simulation of complex pulse pair measurements in (a) rain only with 32 samples and an inherent co-polar correlation coefficient of 0.95 and (b) in rain mixed with melting hail, each with a co-polar correlation coefficient of 0.95, but with an intrinsic differential phase shift of 45° and 50°, respectively

Hydrometeor Classification

fuzzy-logic algorithm

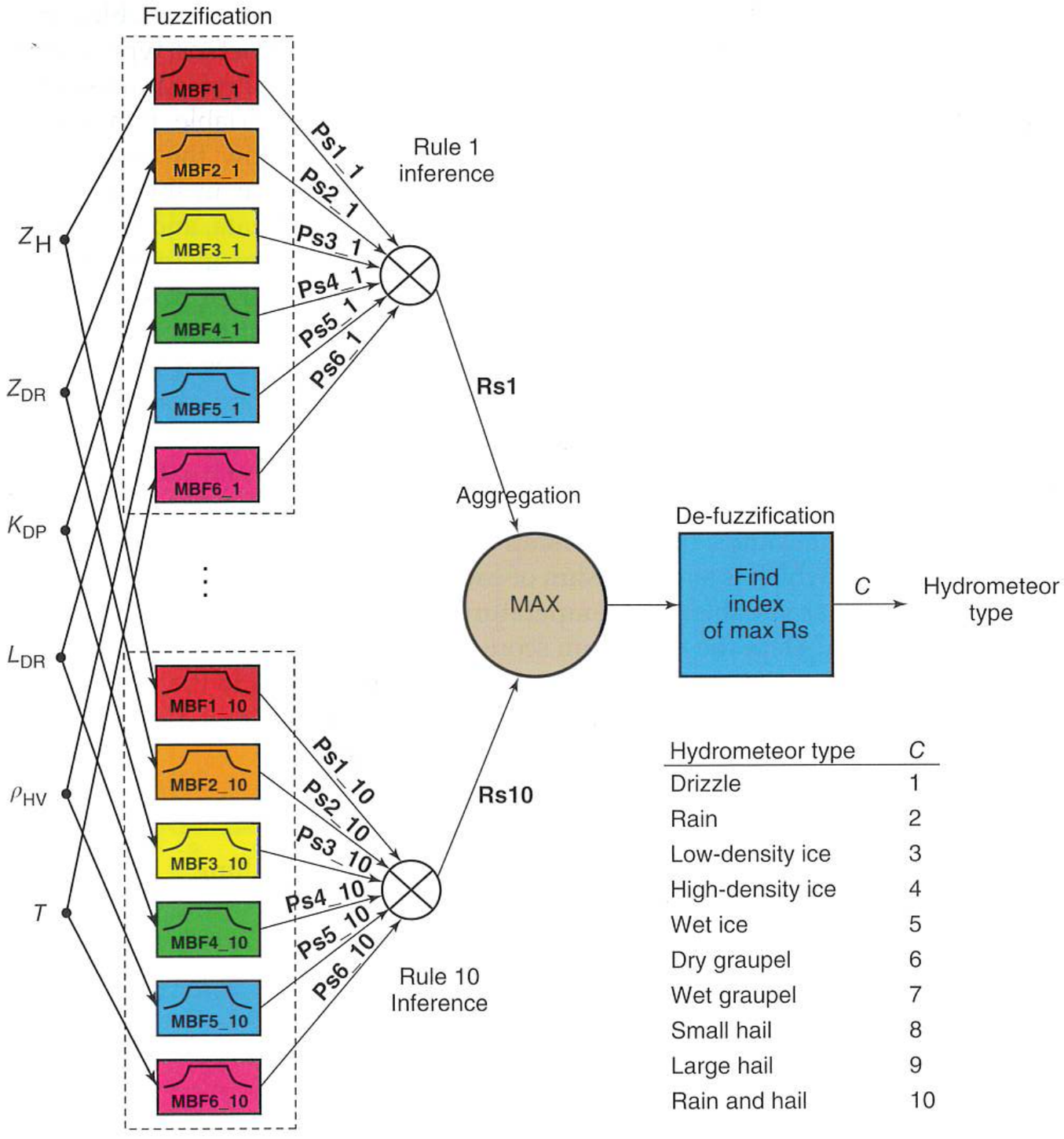

Hydrometeor type	C
Drizzle	1
Rain	2
Low-density ice	3
High-density ice	4
Wet ice	5
Dry graupel	6
Wet graupel	7
Small hail	8
Large hail	9
Rain and hail	10

Figure 7.35 Illustration of a fuzzy logic hydrometeor classification algorithm (Adapted from Liu, H. and Chandrasekar, V. (2000) Classification of hydrometeors based on polarimetric radar measurements: development of fuzzy logic and neuro-fuzzy systems, and *in situ* verification. *J. Atmos. Oceanic Technol.*, **17**, 140–164. © the American Meteorological Society, used with permission)